A Novel Approach to Create a Highly Ordered Monolayer Film of Graphene Nanosheets at the Liquid−Liquid Interface

ARTICLE *in* NANO LETTERS · JANUARY 2009

Impact Factor: 13.59 · DOI: 10.1021/nl802724f · Source: PubMed

NANO LETTERS

Letter

A Novel Approach to Create a Highly Ordered Monolayer Film of Graphene Nanosheets at the Liquid#Liquid Interface

Sanjib Biswas, and Lawrence T. Drzal

Nano Lett., **2009**, 9 (1), 167-172 • DOI: 10.1021/nl802724f • Publication Date (Web): 29 December 2008

NANO LETTERS

2009
Vol. 9, No. 1
167-172

A Novel Approach to Create a Highly Ordered Monolayer Film of Graphene Nanosheets at the Liquid−Liquid Interface

Sanjib Biswas and Lawrence T. Drzal*

Chemical Engineering and Materials Science, Composite Materials and Structures Center, Michigan State University

Received September 8, 2008; Revised Manuscript Received November 26, 2008

ABSTRACT

A monolayer of ultrathin sheets of highly hydrophobic graphene nanosheets was prepared on a large area substrate via self-assembly at the liquid−liquid interface. Driven by the minimization of interfacial energy these planar shaped graphene nanosheets produce a close packed monolayer structure at the liquid−liquid interface. This monolayer film shows high electrical conductivity of more than 1000 S/cm and an optical transmission of more than 70% at a wavelength of 550 nm. Interfacial self-assembly of these nanosheets demonstrates a promising route for the application of this novel material in optoelectronics applications.

Transparent and electrically conductive glasses have a wide range of applications in solar cells, sensor devices, and electrostatic charge dissipating coatings.[1−4] The use of metal oxides like indium tin oxide (ITO) and fluorine tin oxide (FTO) are experiencing limited availability, susceptibility to ion diffusion in polymers and reduced transparency in the infrared (IR) region.[4−6] Carbon nanotubes and graphite oxide nanosheets are possible alternatives to these metal oxides.[7−11] However, these graphite oxide nanosheets require extensive chemical treatment to produce and are electrically nonconductive due to the absence of a delocalized π-electron network on the basal plan.[10−12] The electrical performance of these nanomaterials depends strongly on the relative effectiveness of severe chemical and thermal reductive treatments.[10−12] However, attaining very high electrical conductivity is one of the prerequisites for high performance transparent films.[8] For graphene-based systems, the presence of chemical defects as well as contact resistance over large macroscopic areas are key to the electrical property. While the chemical defects originate from oxidation and reduction of graphite basal plane, the contact resistance over large macroscopic areas depends on the size and the nature of overlaps between the particles within the film. The use of large sized graphene nanosheets with minimum chemical defects into a compact monolayer over a large macroscopic area is therefore promising toward the application of this novel material as transparent conductor.

Exfoliated graphene nanosheets consisting of few layers of graphene, prepared from natural graphite through a simple intercalation and exfoliation process, contain the aromaticity of the graphite basal plane without extensive chemical treatments.[13] The average thickness of these nanosheets can be varied from 3 to 10 nm and the average size can be varied from submicron range to 100 μm.[13] These nanosheets exhibit low electrical resistivity of 50×10^{-6} Ωcm[13] and are also highly hydrophobic. Dispersion of these nanosheets in water results in immediate agglomeration even after sonication.[14,15] The use of surfactants in water shows limited improvement in dispersion quality of these large sized nanosheets.[13] Among the nonpolar solvents, chlorinated liquids like chloroform produce better dispersion. However, conventional drop coating coupled with spin coating or dip coating from chlorinated dispersions results in an irregular structure of agglomerated nanosheets after solvent evaporation.

Directed self-assembly of nano- or microsized particles at the liquid−liquid interface is a potentially alternative approach to fabricate a particle monolayer in regular two-dimensional array in a controllable manner.[16−20] Self-assembly of micrometer sized particles has been demonstrated at the liquid−liquid interface.[27] A reduction in interfacial energy between the oil and water phase drives the particles to assemble at the interface.[16−20] Size dependent self-assembly of hydrophobic CdSe nanoparticles at the liquid−liquid interface was earlier demonstrated by Lin and co-workers.[16] In comparison to microscopic particles, the

* To whom correspondence should be addressed.

10.1021/nl802724f CCC: $40.75
Published on Web 12/29/2008

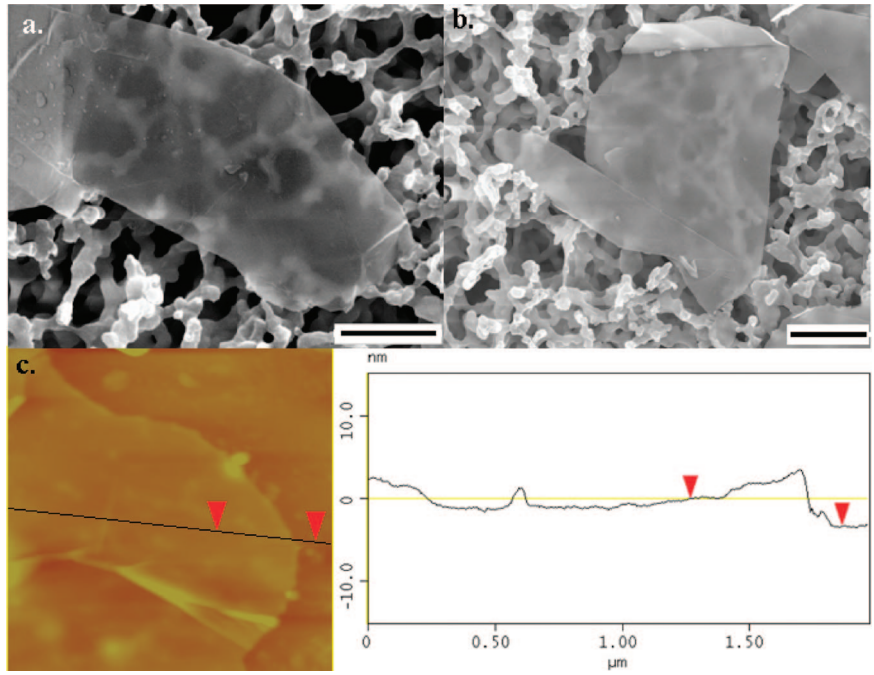

Figure 1. (a,b) FESEM image of graphene nanosheet deposited on cellulose acetate filter membrane. The average size of the nanosheet is estimated to be 8 to 10 μm. The scale bar is 2 μm. (c,d) In the tapping mode AFM image the average thickness of flat nanosheet is 4 nm.

influence of thermal energy on the stability of nanoparticles at the liquid−liquid interface is considerable.[16] A balance between thermal fluctuation and interfacial free energy controls the size and shape selective adsorption of nanoparticles at the liquid−liquid interface.[16−18] At the interface, the difference in wettability of the particle by the two liquid phases can cause the interface to curve around the particle to form a meniscus.[22] The overlap of menisci around each particle generates an attractive lateral capillary force, leading to the formation of a highly ordered particle monolayer at the liquid−liquid interface.[18,22] This research reports on an investigation of the stability and energetically favorable formation of close packed monolayer of highly hydrophobic graphene nanosheets at a liquid−liquid interface and the potential to utilize this approach to produce transparent and electrically conductive monolayer.

Graphene nanosheets were first sonicated in chloroform at a concentration of 0.1 mg/mL. The dispersion was centrifuged for 10 min at 5000 rpm to separate the thinner nanosheets from the semi transparent supernatant liquid at the top. Figure 1a,b shows the field emission scanning electron microscopy (FESEM) image of a typical graphene nanosheet deposited on a cellulose acetate filter membrane from the centrifugally separated chloroform dispersion. The average size of the nanosheet is estimated to be 8 to 10 μm. The average thickness of the starting graphene nanosheets was previously estimated to be less than 10 nm.[13] However, after the separation of the thinner nanosheets by centrifuging, AFM was used to measure the thickness of individual nanosheets. Figure 1c shows that the average nanosheet thickness is 3 to 4 nm. However, it should be noted that nanosheets are not completely lying flat on the substrate and thus there are some variations in the height.

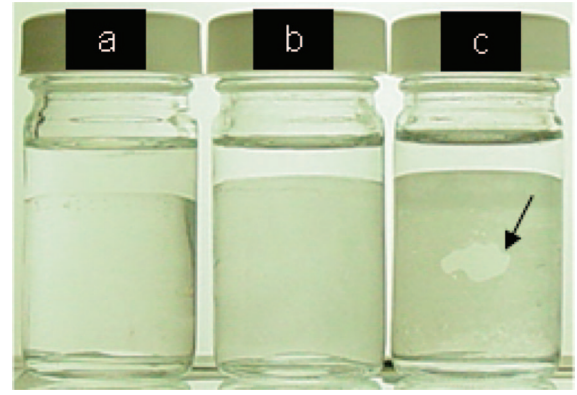

Figure 2. Adsorption of graphene nanosheets at the liquid interface. (a) Distinct phases of two pure liquids, chloroform and water, in contact with each other. (b) Graphene nanosheets are dispersed in the chloroform phase and water is added on the top to get two distinct phases with graphene nanosheets dispersed in the chloroform phase. This two-phase mixture is then briefly sonicated to adsorb the nanosheets at the liquid−liquid interface. (c) Film of graphene nanosheets covering the liquid−liquid interface and then extending up the chloroform glass interface. On the marked area of panel c, a part of the film has been cracked with a spatula to show the liquid inside.

Figure 2 illustrates various steps to produce the two-dimensional arrays of graphene nanosheets at the liquid−liquid interface. The first nanosheets are dispersed in chloroform, and after water is added to the mixture two distinct phases formed containing graphene nanosheets dispersed in the chloroform phase. However, to transport the nanosheets completely from the bulk phase to the liquid−liquid interface requires an input of mechanical work through sonication for a brief period of time. The external mechanical force breaks

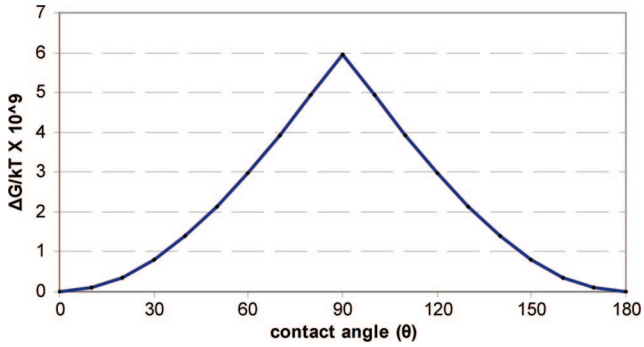

Figure 3. Free energy of particle detachment. The above figure shows the variation in free energy of detachment of particle as a function of contact angle (θ). The particle thickness and width are 4 nm and 10 μm, respectively.

the two immiscible liquid phases into numerous drops and bubbles creating a large interfacial area between the two liquids. Driven by the minimization of interfacial free energy, the graphene nanosheets are preferentially adsorbed at the chloroform-water interface.

However, interfacial adsorption of particles at the interface reduces the entropy by the Boltzmann factor.[16−18,21,22] Therefore the gain in the interfacial energy is responsible for the stability of the particles at the interface.[16−18,21,22] The three interfacial energies at the particle-oil interface γ_{po}, particle−water interface γ_{pw}, and oil−water interface γ_{ow} are related to each other through the three phase contact angle by the Young's equation as[23]

$$\cos\theta = (\gamma_{po} - \gamma_{pw})/\gamma_{ow}$$

Apart from the three interfacial energies, the role of particle size and shape are paramount to the gain in the total interfacial energy of the system. Following an analysis, developed by Binks, the energy of attachment of the disk- or flat-shaped particle over various contact angles at the liquid−liquid interface can be analyzed.[21] In contrast to spherical nanoparticles, a disk- or plate-shaped particle, such as this graphene nanosheet is characterized by two different axes. The longer axis is along the width of the nanosheet and the aspect ratio "*a*/*b*" is thus the ratio of two axes along the width and thickness of the nanosheets. With the thickness and average width of the nanosheets taken as 4 nm and 10 μm, respectively, the aspect ratio *a*/*b* is 2500. Assuming that particles are attached to a planar oil−water interface, the free energy of detachment of a planar nanosheet into the water and the chloroform phase is given as

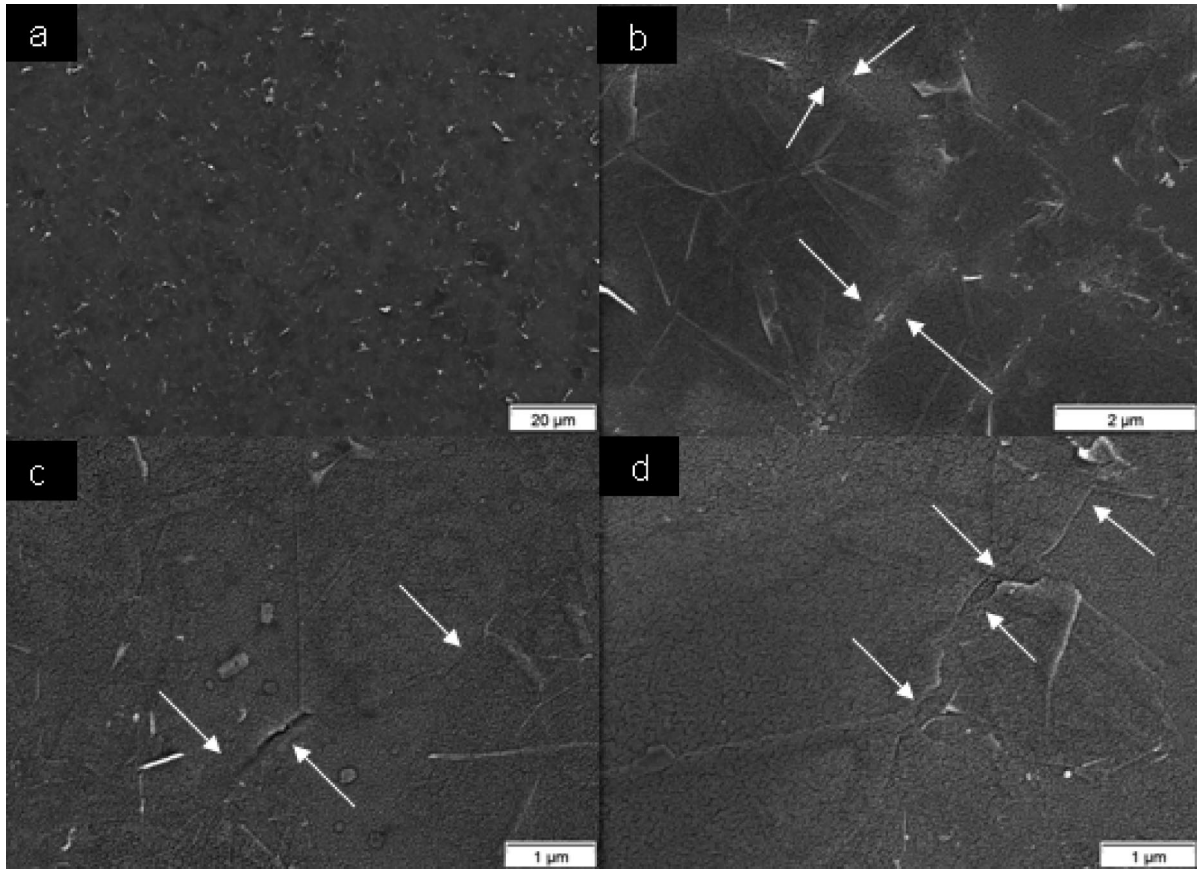

Figure 4. Monolayer film of graphene nanosheets. (a−d) FESEM micrographs of graphene nanosheets deposited on the glass slide. The specimen was sputter coated with gold to get better contrast on the image. Images, taken from different areas, clearly exhibit how the planar nanosheets are interconnected with each other. Without coming on top of each other, nanosheets are well interconnected, forming a monolayer over the large area of the substrate. The arrows, shown in the images, indicate the edge of nanosheets.

$$\Delta G_{dw} = \gamma_{ow}\pi b^2(1-\cos\theta)^2[1+(a/b-1)^2/(1-\cos\theta)+ 2(a/b-1)(\sin\theta-\theta\cos\theta)/(1-\cos\theta)^2] \quad \text{(i)}$$

$$\Delta G_{chl} = \Delta G_{dw} + 2\pi\gamma_{ow}b^2\cos\theta[(a/b-1)^2+\pi(a/b-1)+2] \quad \text{(ii)}$$

Where, ΔG_{dw} and ΔG_{chl} are the free energies of detachment of the particle from the interface into the water and the chloroform phase respectively. "γ_{ow}" is the interfacial energy at the chloroform water interface. Equation i describes the free energy of detachment of the particle into the water phase at contact angle between 0 to 90° and eq ii corresponds to the free energy of detachment of the particle into the chloroform phase at contact angle between 90 to 180°. The free energy of particle detachment as compared to the thermal energy at various contact angle θ is shown in Figure 3.

At equilibrium, free energy of attachment of the particle to the liquid−liquid interface is $\Delta G_a = -\Delta G_d$. With the measured three phase contact angle between water and chloroform on the graphene nanosheet close to 94°, the above calculation predicts that the particle attachment at the liquid−liquid interface is energetically highly favorable. Therefore, the larger and thinner the nanosheet, the higher would be the aspect ratio, and it is more favorable for the nanosheets to get adsorbed at the interface with substantial gain in the interfacial energy.

In natural graphite, the layers of graphene are strongly attached to each other by van der Waals force of attraction. The cohesive energy was determined to be 5.8 kJ/mol with each layer separated by a distance of 3.36 Å.[24−26] After intercalation and exfoliation, these layers are separated from each other. However, the attractive interaction energy between the graphene nanosheets is strong. In this study, the thinner nanosheets of graphene, separated by centrifugation in chloroform, is very stable for days without any visible settling keeping the individual nanosheets separated from each other. Introduction of the water phase and subsequent sonication produces a large interfacial area between these two immiscible liquids. At this point, the nanosheets gain interfacial free energy by adsorption at the liquid−liquid interface rather than restacking and settling out of the suspension. Thus with increasing concentration, nanosheets are expected to concentrate at the liquid−liquid interface. Experimentally it was found that with increasing nanosheet concentration the extent of the interfacial adsorption area covered with the nanosheets increased. The graphene nanosheet film extended downward toward the edge of the chloroform phase with a thin layer of water outside (Figure 2c). However, at higher concentration, thick layers of nanosheets were found near the interface resulting in agglomeration and coalescence. Thus, while the gain in interfacial energy drives nanosheets to form a monolayer at the liquid−liquid interface, the concentration

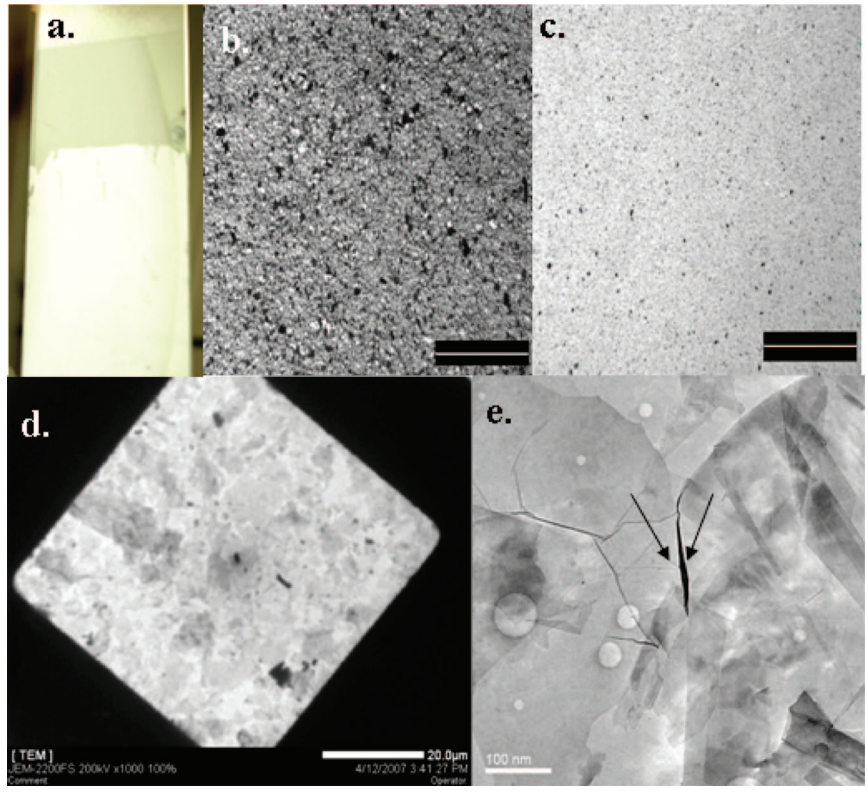

Figure 5. (a) The metallic luster of graphene nanosheet film under white light. The film is deposited on microscopic glass slide. (b,c) Optical microscopy images of film prepared from two different nanosheet thicknesses. Numerous dark spots in panel b give clear evidence of the presence of thicker nanosheets of average thickness of 10 nm. Under similar condition, film prepared from thinner nanosheets of an average thickness of 3 to 4 nm shows much higher transparency as shown in panel c. The scale bar is 500 μm. (d) Low-magnification TEM image. (e) High-magnification TEM micrograph explains the morphology of the film with individual nanosheets touching each other at the edges without any complete overlap. The arrows on the image 5e indicate how two individual nanosheets are interconnected through the edges.

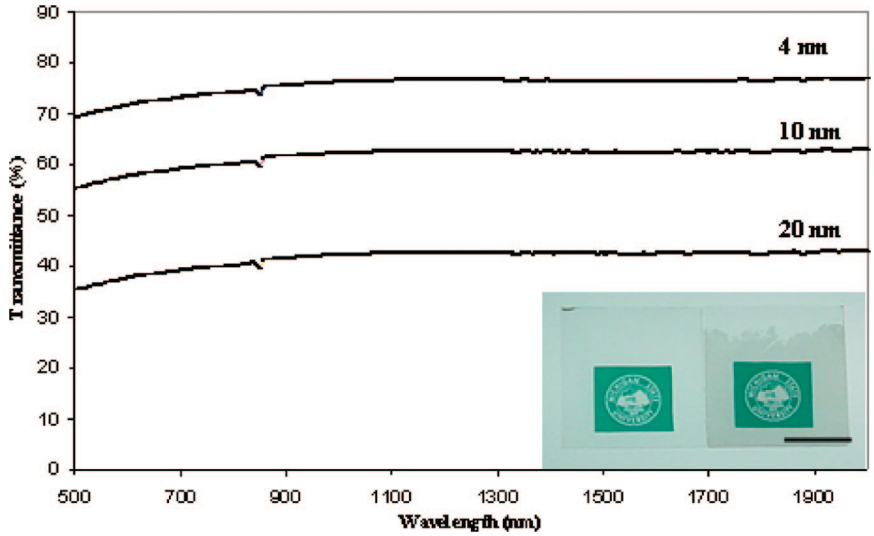

Figure 6. Optical transmission spectra. Optical transmission spectra from 500 to 2000 nm of monolayer film of graphene nanosheets at various nanosheet thicknesses. Inset, the photograph illustrates the clarity and transparency of a 4 nm thickness graphene nanosheet film. The scale bar is 1 in.

of the nanosheets must be controlled to prevent nanosheet agglomeration and coalescence.

The thin graphene nanosheet film formed at this liquid−liquid interface was transferred onto a glass substrate and the morphology and orientation of the graphene nanosheets were characterized by the high resolution FESEM imaging. Representative images taken from different sections of the film are shown in Figure 4. From the FESEM characterization, it is evident that the graphene nanosheets form a close packed array with remarkable uniformity over a macroscopic sized area. The graphene nanosheets are well dispersed and interconnected at the edges with little detectable gaps. Furthermore, there was very little overlapping of the graphene nanosheets observed.

The metallic luster of the graphene nanosheet film, as shown in figure 5a, indicates a close-packed structure over large macroscopic area. The formation of compact monolayer structure was further evident from the optical microscopy image of films prepared from two different nanosheet thicknesses. The darker regions in the optical micrograph of Figure 5b represent film prepared from nanosheets with an average thickness of 10 nm. Under similar measurement condition, films prepared from nanosheets with an average thickness of 3 to 4 nm show high transparency over a large macroscopic area as shown in Figure 5c. A complete overlap between thinner nanosheets in Figure 5c would have resulted in reduced transparency as shown in Figure 5b. This result substantiates the fact that individual adsorption of the nanosheets at the liquid−liquid interface is energetically more favorable than restacking and agglomerating with each other. Low- and high-magnification transmission electron microscopy (TEM) images in Figure 5d,e also reveal a compact monolayer structure with two individual nanosheets touching each others at the edges as shown in Figure 5e.

Thus the above investigations from FESEM, TEM, and optical microscopy suggests that once the minimization of interfacial energy drives the nanosheets from the bulk phase to the liquid−liquid interface, they self-assemble as a result of force of interaction between them to create a large area close packed monolayer structure.

These graphene nanosheets are highly hydrophobic. However, a very small amount of oxygen functional groups always covers the edge of the nanosheet.[13] Therefore, it is expected that the presence of both hydrophobic and hydrophilic faces at the edge of the nanosheet can perturb the interface large enough to generate a menisci around the particle.[22,27] Attractive lateral capillary force generates from the overlap of such "like" menisci around the particle to form a close-packed structure at the liquid−liquid interface.[22] Directed self-assembly through the formation of "capillary bond" for particles with both hydrophilic and hydrophobic faces was demonstrated earlier.[27,28] While the magnitude of this lateral capillary force is negligible for spherical particles with diameter less than 10 μm,[29] previous work from Bowden et al. showed that for planar-shaped particles at the liquid−liquid interface, the lateral capillary force is quite significant even for particles with thicknesses of few nanometers.[18] They analyzed the lateral capillary force as the two bodies approach each other from infinite distance. As the two bodies approach each other, the height of the meniscus is related to the change in the arc length. The interfacial energy is then obtained by multiplying the change in arc length, the interfacial tension between two liquids and the aspect ratio of the nanosheet. Following this same approach, calculation of the interfacial free energy shows that the capillary force driven two-dimensional self-assembly of graphene nanosheets is energetically favorable with a ΔG of more than $-10\ k_BT$ at nanosheet thickness of 4 nm with an aspect ratio of 2500. As a result this capillary force drives the graphene nanosheets to each other maximizing their hydrophobic surface area and creating a close packed monolayer at the liquid−liquid interface in exact agreement with our observation and measurement.

Graphene nanosheet film transparency was measured at various film thicknesses. The thickness of the nanosheet depends on the surface area of the parent exfoliated graphene

nanosheet. We separated thin sheets of graphene from exfoliated graphene nanosheet with different surface areas. With low surface area materials, the transparency of the film is as low as 10%. With increasing surface area, the thickness of the nanosheet decreases and the transparency of the corresponding film increases. Figure 6 represents the optical transmission profile of graphene nanosheet film obtained from different thickness nanosheets. At a wavelength of 500 nm the transmission of graphene nanosheet film having an average thickness of 4 nm is about 70%. The transmission increases to slightly less than 80% at increasing wavelength. In a recent publication by Hersam et al., a similar transparency at 500 nm wavelength was achieved by using high-purity metallic carbon nanotubes.[8] The transmission characteristics are very flat in the visible and near-infrared region of the electromagnetic spectrum to 2000 nm in contrast to the ITO- and FTO-coated glass. This result is consistent with previously published reports on reduced graphite oxide films.[10−12] Such an optical transmission profile makes these types of graphene films highly desirable for optoelectronics applications. Recently research was reported in which a measurement on a single layer of graphene was conducted and 2.3% absorption of incident white light was measured.[30] With an average nanosheet thickness of 3 to 4 nm in our experiments, we achieved a transparency close to 70%, which based on the thckness of our nanosheets agrees with and is in direct proportion to the 2.3% adsorption per layer of graphene.

The electrical conductivity of the graphene nanosheet film was measured by using the four point probe method at 10 different locations on the film. The average sheet resistance of the graphene nanosheet film of 4 nm thickness is 10^2 Ω/sq and the average conductivity is more than 1000 S/cm. The highest electrical conductivity was near 1250 S/cm. This high value of electrical conductivity is comparable with FTO-coated glass slides as well as transparent carbon nanotube electrodes.[4,7−9] However, compared to the conventional metal oxides like ITO or FTO, this monolayer film is thermally very stable. After heating a specimen at 350 °C for more than 3 h in an ambient atmosphere, the conductivity of the film did not change. In contrast to a published report on the graphene nanosheet films made from reduced graphite oxide,[10−12] the electrical conductivity of this graphene nanosheet film is independent of the film thickness. The average film conductivity is always more than 1000 S/cm regardless of film thicknesses. This observation is consistent with the fact that these nanosheets form a close-packed monolayer at the liquid−liquid interface. This close-packed structure ensures high electrical conductivity irrespective of the thickness of the nanosheet.

Previous research[10−12] has produced ultrathin layers of graphene using the graphite oxide route allowing water-based processing but requiring the use of hazardous chemicals to produce graphite oxide and to reduce it back to graphene. This research has shown that the highly hydrophobic nature of the graphene nanosheet can be used to self-assemble thin graphene nanosheet at the hydrophobic liquid−hydrophilic liquid interface into a close packed monolayer. As a result the native properties of graphene are preserved without requiring chemical transformation of the basal plane. The resulting graphene nanosheet monolayer film is highly compact, optically transparent from the visible to the infrared region and electrically conductive. The large microscopic size of the graphene nanosheets that comprise the film reduces the contact resistance over the macroscopic area of the film. The graphene nanosheets are inexpensive to produce and the process to form a monolayer is easily scalable to very large areas offering a new material and method to replace ITO and FTO coatings for optoelectronics applications.

References

(1) Gan, Y.; Liu, J.; Zeng, S. *Surf. Coat. Technol.* **2006**, *201*, 25–29.
(2) Rowell, M. W.; Topinka, M. A.; McGeheea, M. D.; Prall, H.-J.; Dennler, G.; Sariciftci, N. S.; Hu, L.; Gruner, G. *Appl. Phys. Lett.* **2006**, *88*, 233506−1–3.
(3) Schmidt-Mende, L.; Fechtenkotter, A.; Mullen, K.; Moons, E.; Friend, R. H.; MacKenzie, J. D. *Science* **2001**, *293*, 1119–1122.
(4) Andersson, A.; Johansson, N.; Bröms, P.; Yu, N.; Lupo, D.; Salaneck, W. R. *Adv. Mater.* **1998**, *10*, 859–863.
(5) Schlatmann, A. R.; Floet, D. W.; Hilberer, A.; Garten, F.; Smulders, P. J. M.; Klapwijk, T. M.; Hadziioannou, G. *Appl. Phys. Lett.* **1996**, *69*, 1764–1766.
(6) Lee, S. T.; Gao, Z. Q.; Hung, L. S. *Appl. Phys. Lett.* **1999**, *75*, 1404–1406.
(7) Wu, Z.; Chen, Z.; Du, X.; Logan, J. M.; Sippel, J.; Nikolou, M.; Kamaras, K.; Reynolds, J. R.; Tanner, D. B.; Hebard, A. F.; Rinzler, A. G. *Science* **2004**, *305*, 1273–1276.
(8) Green, A. A.; Hersam, M. C. *Nano Lett.* **2008**, *8*, 1417–1422.
(9) Shim, B. S.; Tang, Z.; Morabito, M. P.; Agarwal, A.; Hong, H.; Kotov, N. A. *Chem. Mater.* **2007**, *19*, 5467–5474.
(10) Wang, X.; Zhi, L.; Mullen, K. *Nano Lett.* **2008**, *8*, 323–327.
(11) Becerril, H. A.; Mao, J.; Liu, Z.; Stoltenberg, R. M.; Bao, Z.; Chen, Y. *ACS Nano* **2008**, *2*, 463–470.
(12) Eda, G.; Fanchini, G.; Chhowalla, M. *Nat. Nanotechnol.* **2008**, *3*, 270–274.
(13) Fukushima, H. *Graphite Nanoreinforcements in Polymer Nanocomposites*. Ph.D. Dissertation, Michigan State University, East Lansing, MI, 2003..
(14) Hendricks, T. R.; Lu, J.; Drzal, L. T.; Lee, I. *Adv. Mater.* **2008**, *20*, 2008–2012.
(15) Lu, J.; Drzal, L. T.; Worden, R. M.; Lee, I. *Chem. Mater.* **2007**, *19*, 6240–6246.
(16) Lin, Y.; Skaff, H.; Emrick, T.; Dinsmore, A. D.; Russell, T. P. *Science* **2003**, *299*, 226–229.
(17) Binder, W. H. *Angew. Chem., Int. Ed.* **2005**, *44*, 5172–5175.
(18) Bowden, N.; Terfort, A.; Carbeck, J.; Whitesides, G. M. *Science* **1997**, *276*, 233–235.
(19) Duan, H.; Wang, D.; Kurth, D. G.; Mohwald, H. *Angew. Chem., Int. Ed.* **2004**, *43*, 5639–5642.
(20) Wang, D.; Duan, H.; Mohwald, H. *Soft Matter* **2005**, *1*, 412–416.
(21) Binks, B. P. *Colloidal particle at liquid interfaces*; Cambridge University press: New York, 2006.
(22) Kralchevsky, P. A.; Nagayama, K. *Particle at fluid interfaces and membranes*; Elsevier: New York, 2001.
(23) Stokes, R. J.; Evans, D. F. *Fundamentals of Interfacial Engineering*; Wiley-VCH: New York, 1996.
(24) Palser, A. H. R. *Phys. Chem. Chem. Phys.* **1999**, *1*, 4459–4464.
(25) Girifalco, L. A.; Lad, R. A. *J. Chem. Phys.* **1956**, *25*, 693–697.
(26) Si, Y.; Samulski, E. T. *Nano Lett.* **2008**, *8*, 1679–1682.
(27) Bowden, N.; Arias, F.; Deng, T.; Whitesides, G. M. *Langmuir* **2001**, *17*, 1757–1765.
(28) Bowden, N.; Oliver, S. R. J.; Whitesides, G. M. *J. Phys. Chem. B* **2000**, *104*, 2714–2724.
(29) Kralchevsky, P. A.; Paunov, V. N.; Denkov, N. D.; Ivanov, I. B.; Nagayama, K. *J. Colloid Interface Sci.* **1993**, *155*, 420.
(30) Nair, R. R.; Blake, P.; Grigorenko, A. N.; Novoselov, K. S.; Booth, T. J.; Stauber, T.; Peres, N. M. R.; Geim, A. K. *Science* **2008**, *320*, 1308.

NL802724F